Atmos. Meas. Tech. Discuss., 8, 7455–7489, 2015
www.atmos-meas-tech-discuss.net/8/7455/2015/
doi:10.5194/amtd-8-7455-2015

Atmospheric Measurement Techniques Discussions

Long term validation of ESA operational retrieval (version 6.0) of MIPAS Envisat vertical profiles of methane, nitrous oxides, CFC-11 and CFC-12 using balloon borne observations and trajectory matching

A. Engel[1], H. Bönisch[1], T. Schwarzenberger[1,a], H. P. Haase[1,b], K. Grunow[2,c], J. Abalichin[2], and S. Sala[1,d]

[1]Institute for Atmospheric and Environmental Sciences, Goethe Universität, Frankfurt, Germany
[2]Institut für Meteorologie, Freie Universität Berlin, Berlin, Germany
[a]now at: Technologiezentrum Wasser, Karlsruhe, Germany
[b]now at: Deka Bank, Frankfurt, Germany
[c]now at: Senatsverwaltung für Stadtentwicklung und Umwelt, Berlin, Germany
[d]now at: Deutscher Wetter Dienst, DWD, Offenbach, Germany

Received: 18 May 2015 – Accepted: 15 June 2015 – Published: 21 July 2015

Correspondence to: A. Engel (an.engel@iau.uni-frankfurt.de)

Published by Copernicus Publications on behalf of the European Geosciences Union.

AMTD
8, 7455–7489, 2015

Abstract

MIPAS-Envisat is a satellite-borne sensor which was measuring vertical profiles of a wide range of trace gases from 2002 to 2012 using IR emission spectroscopy. We present geophysical validation for the operational retrieval (version 6.0) of N_2O, CH_4, CFC-12 and CFC-11 by the European Space Agency (ESA) of MIPAS-Envisat. The geophysical validation data are derived from measurements of samples collected by a cryogenic whole air sampler flown to altitudes of up to 34 km by means of large scientific balloons. In order to increase the number of coincidences between the satellite and the balloon observations we applied a trajectory matching technique. The results are presented for different time periods due to a change in the spectroscopic resolution of MIPAS as of early 2005. Retrieval results for N_2O, CH_4 and CFC-12 show partly good agreement for some altitude regions, which differs for the periods with different spectroscopic resolution. However, significant differences to the balloon data are also observed for some altitude regions, which depend on species and spectroscopic resolution. These differences need to be considered when using these data. The CFC-11 results from the operation retrieval version 6 cannot be recommended for scientific studies due to a systematic overestimation of the CFC-11 mixing ratios.

1 Introduction

Measurements of long lived traces gases in the stratosphere serve a variety of purposes. They can be used to determine relative lifetimes (Plumb and Ko, 1992), to observe dynamical processes, to study transport time scales, the so called mean age and also to derive chemical budgets. For some of these studies relative changes and gradients of trace gases are used, but for the most part high precision and accuracy are needed to derive quantitative information. In-situ observations in the stratosphere, which can be conducted from high flying aircrafts up to altitudes of 20 km and from large scientific balloons for altitudes up to 40 km often provide information on tracers

AMTD
8, 7455–7489, 2015

of interest at high resolution and high accuracy. The information obtained is however very sparse in space and time. On the other hand, satellite borne sensors often provide very good temporal and spatial coverage yet the vertical resolution is limited and the accuracy and precision of satellite observations are critical factors, which need to be evaluated carefully. A comparison of the high accuracy in-situ observations with satellite data retrievals is necessary to estimate the quality of satellite data and to identify possible biases.

As mentioned above, the density of satellite observations is often much higher than that of the respective in-situ data to be used for the validation. During the acquisition of the in-situ validation data care can be taken to achieve a good match in time and space to the satellite observations. However, this can only be achieved for one single vertical profile. It is however desirable to use the valuable in-situ data for validation of more than only one satellite profile. For this purpose either climatological approaches or tracer-tracer correlations can be used. Another approach is the use of trajectories to find more incidences during which the satellite measured the same air parcel as the in-situ observations.

Here we present work on validation of long lived traces gases N_2O, CH_4, CFC-12 and CFC-11 derived from observations of the MIPAS Fourier Transform InfraRed (FTIR) spectrometer on board the Envisat satellite. Previous results on the validation of different data products for these gases have been published (Hoffmann et al., 2008; Kellmann et al., 2012; Payan et al., 2009; Vigouroux et al., 2007) and the data have been used e.g. to derive stratospheric lifetimes (Engel and Atlas et al., 2013; Minschwaner et al., 2013) and climatologies and trends of CFC-11 and CFC-12 (Kellmann et al., 2012). While MIPAS is not operating anymore, it has provided a wealth of data for about 10 years. A thorough validation of these data is the prerequisite for their scientific application. Here we present a comparison of measurements of long lived trace gases obtained using a cryogenic whole air sampler and the data set from the operational ESA retrieval version ML2PP/6.0. In order to enhance the number of coincidences between the in-situ observations and the satellite data set we apply trajectory map-

AMTD
8, 7455–7489, 2015

ping techniques. This technique and the different data sets are described in Sect. 2. In Sect. 3, we present the results for the four trace gases N_2O, CH_4, CFC-12 and CFC-11, which are then summarized and discussed in Sect. 4.

2 Data sets

2.1 MIPAS-E Michelson Interferometer of passive atmospheric sounding

The Michelson Interferometer for Passive Atmospheric Sounding (MIPAS) is an emission spectrometer measuring atmospheric trace gases in the mid-infrared region using Fourier Transform spectroscopy (Fischer et al., 2008). MIPAS was operated on different platforms. The satellite version on board the Envisat satellite operated by the European Space Agency (ESA) provided data for a large number of atmospheric trace gases from March 2004 until the end of operation in April 2012. The limb scanning geometry allows to combine high vertical resolution of up to 3 km and good global coverage with about 1000 vertical profiles per day. Vertical profiles in so-called nominal mode are retrieved for about 16 tangent altitudes in a range between 8 and 68 km. The data are processed by ESA in a near operational way for a limited number of trace gases. In addition the data are evaluated for a number of scientific data products (e.g. Kellmann et al., 2012; Stiller et al., 2008). The original spectral resolution was 0.035 cm^{-1}, which had to be reduced to 0.0625 cm^{-1} due to problems with the scanning mirror. The data set starting in January 2005 is based on these lower resolution data. Due to this change in resolution the validation results are presented separately for the time period prior to 2005 (high resolution data in the following) and the data after January 2005 (low resolution data in the following).

2.2 The cryogenic whole air sampler BONBON

The cryogenic whole air sampler (cryosampler) BONBON is an instrument designed for collection of large whole air samples during the flight of large stratospheric balloons.

AMTD
8, 7455–7489, 2015

The instruments carries 15 internally electropolished stainless steel canisters which can be opened and closed at different altitudes. The sample canisters are cooled to 27 K using liquid Neon. At this temperature the ambient air will condense on the inner surfaces of the sample canisters allowing to collect very large air samples corresponding to up to 15 L at standard temperature and pressure, during rather short times. E.g. at 30 km the time to collect such a large sample is typically below 5 min. The samples are typically collected during the valve controlled slow descent of the balloon at vertical velocities of 2–3 m s^{-1}. A 5 min sampling interval will thus result in 750 m vertical resolution. Depending on the external pressure, sampling time and vertical velocities the vertical resolution is usually between 100 m and 1 km. More details on the technique of cryogenic whole air sampling can be found in (Lueb et al., 1975) and on the cryosampler used for this study in (Engel et al., 1997).

The samples are subsequently analysed in the laboratory using a variety of gas chromatographic methods and reported on internationally accepted calibration scale. In this paper, data for the trace gases N_2O, CH_4, CFC-12 and CFC-11 are compared. N_2O and CH_4 were measured at the University of Heidelberg by gas chromatography with electron capture (Schmidt et al., 2001) and flame ionization (Levin et al., 1999) detection respectively. N_2O was in addition also measured at University Frankfurt. The data used for the intercomparison are those from University of Frankfurt except for flight B46 where N_2O data from University of Heidelberg are used. The chlorofluorocarbons CFC-11 and CFC-12 were measured at University Frankfurt by gas chromatography coupled to mass-spectrometry (Hoker et al., 2014; Laube et al., 2008), with the exception of the measurements prior to 2004 which were made using electron capture detectors (Engel et al., 1997). N_2O is reported on the NOAA 2006 scale for all observations (Hall et al., 2007), CH_4 on the NOAA 2004 (Dlugokencky et al., 2005) scale and the CFC-11 and CFC-12 are reported relative to the NOAA 1993 and 2001 scales (Montzka et al., 2003), respectively. Typical reproducibilities for these four substances are 0.5–1 % (CFC-11), 0.5 % (CFC-12), 0.2 % (CH_4) and 0.5 % (N_2O). Absolute accuracies of the calibration scales are 1 % or less for all species. As these uncertainties are

AMTD
8, 7455–7489, 2015

much smaller than those of the satellite sensors they are neglected in the discussion of the validations results.

2.3 Available validation flights

A total of 7 flights of our cryogenic whole air sampler have been carried out during the time that MIPAS-E was operational. Not all flights were explicitly for the purpose of validation resulting in different quality of the direct coincidence with MIPAS-E observations. The flights took place at different latitudes ranging from the tropics (5° S) to the high northern latitudes (68° N) under different meteorological conditions and during different seasons. The dates, launch locations, latitudes and altitude ranges covered by the flights are shown in Table 1.

In the following we will give some very brief information about the individual flights. Flight B39 was launched from southern France in fall 2002 and represents typical undisturbed conditions during the turnaround from summer to winter circulation at the mid latitudes of the Northern Hemisphere. Flight B40 was launched from the high latitude site of ESRANGE near Kiruna in northern Sweden during the polar winter. Some very low mixing ratios where observed inside the polar vortex due to the well-known effect of diabatic descent inside the vortex. This flight is discussed in detail in (Engel et al., 2006), in particular with respect to the intrusion of mesospheric air into the stratosphere. A further flight (B41) was launched to probe the high latitude stratosphere during summer. Flight B42 and B43 were launched from Teresina in Brazil (5° S) to probe the stratosphere in the inner tropics. The vertical profiles of many trace gases show much smaller decrease with altitude in the lower tropical stratosphere and then steep gradients with altitude inside the loss regions for the specific substances. These two flight are discussed in more detail in (Laube et al., 2008). The two most recent flights are again from high northern latitudes during winter and were launched on 9 March 2009 (B45) and 1 April 2011 (B46) respectively. The flight B45 mainly sampled air from outside the polar vortex, with the exception of a tongue of vortex air sampled between about 20 and 25 km altitude. The flight B46 was launched very close to the edge of

AMTD
8, 7455–7489, 2015

the polar vortex which was unusually strong and showed very high wind speeds at the edge during this year (see e.g. Manney et al., 2011). Due to these unusually strong horizontal winds only a very short flight could be carried out and the maximum altitude reached was only 23 km. The observed mixing ratios of the long lived tracers are typical of conditions at the inner edge of the polar vortex with rather low mixing ratios close to those observed well inside the vortex.

2.4 Trajectory matching and data handling

As mentioned above the amount of satellite data which can be compared by a direct match is very limited and usually consists of only one or two scans of the satellite instrument. In order to enhance the number of satellite vertical profiles which can be used for the intercomparison we have applied the technique of trajectory mapping using the University of Berlin trajectory model (Grunow, 2009; Naujokat and Grunow, 2003). Trajectories are initiated about every 200 m in altitude (for flights prior to 2009) or every 10 s, i.e. about every 20–50 m (for flight in 2009 and 2011) along the flight path of the balloon and run forward and backward in time for five days (Grunow, 2009). All MIPAS-E observations which are within a 500 km radius and a 1 h time mismatch with the trajectory are regarded as having sampled the same air mass. In addition only matches are used in this study where at least 4 trajectories fulfill the match criteria and the matched altitude interval of the satellite profile is more than 1.5 km (Schwarzenberger, 2014).

The trajectory calculations were performed on potential temperature surfaces and vertical displacement in potential temperature space was taken into account using climatological heating rates (Grunow, 2009). As trajectories are not calculated for more than 5 days in general this only leads to very small deviations in the matches from trajectories using explicitly calculated heating rates (Grunow, 2009). For clarity the results are presented on an altitude scale, which is that of the balloon profile along which the trajectories were initiated. This altitude is based on GPS measurements. For the flights prior to 2009 operational ECMWF data on 2.5° × 2.5° grid were used, while the calcu-

AMTD
8, 7455–7489, 2015

lations for the flights in 2009 and 2011 are based on 1.25° × 1.25° operational ECMWF data. The trajectory model is run using 25 vertical levels for the 2.5° × 2.5° grid data and 59 levels for the 1.25° × 1.25° grid data.

For a comparison with the balloon observations the matched satellite data points were averaged over 1 km intervals. For the quantitative intercomparison the balloon observations are then interpolated to the mean potential temperature of the matched satellite data. Again, for clarity the results are reported on an altitude scale based on the balloon trajectory, while the calculation of the matches is based on potential temperature.

3 Validation results

In the following we present the validation results for the four species mentioned above. Results are only shown for the version 6.0 of the operational ESA data retrieval. Measurements of the four trace gases are available for all samples collected with the cryogenic whole air sampler. We present the results for all species separately. The direct comparison of the vertical profile gives a qualitative impression of the quality of the intercomparison. For each species we present the direct comparison on an altitude vertical scale from flight B45 launched on 10 March 2009 from the Esrange near Kiruna, as this flight covers a large altitude range and a wide range of mixing ratios. It also shows a sharp structure which is in particular challenging for satellite validation and shows the limitations of the method applied here.

For a more quantitative comparison the information from several flights is combined. For this purpose the in-situ measurements are interpolated in altitude to give a value at the same altitude as the mean altitude of the MIPAS-E data in the respective bin. Results are separated for the period up to 2005 (high resolution) and for the period with lower spectral resolution of MIPAS-E starting in January 2005. We have chosen 1 km intervals for the binning of MIPAS-E data. As noted above the uncertainty in the in-situ is sufficiently small to be neglected in comparison to the uncertainty of the satel-

AMTD
8, 7455–7489, 2015

lite data. As a number of satellite data points is averaged in each bin, there are two sources of uncertainty which have to be considered for this intercomparison. One is the uncertainty of an individual measurement point as specified from the retrieval algorithm and the other is the variability of the individual data points in the bin around the mean value. For the direct comparison the error given for the MIPAS-E data is the standard deviation of the data points in the respective bin, it is thus the variability of the retrieved values. In case there are no systematic deviations it is expected that the MIPAS-E data should scatter around the in-situ data. For the quantitative comparison two error bars are given. The ones in red are the same as those given in the direct comparison, while the blue lines show the mean of the uncertainty quoted in the data files. This representation will thus show whether the uncertainty given in the datafiles is representative for the mean deviation between satellite data and in-situ measurements.

3.1 MIPAS-E-CH_4

In Fig. 1 a direct comparison of the methane profile obtained from the cryosampler flight on 10 March 2009 (Flight B45) with the matched MIPAS-E values based on the version 6 ESA retrieval is shown. Below 20 km an excellent agreement is observed. Above 25 km for the validation based on B45 good agreement of the MIPAS-E retrieval and balloon data is observed which agrees within the scatter of the MIPAS-E data. The sharp structure observed between 20 and 25 km cannot be reproduced by the satellite observations. There is however an enhanced variability of the MIPAS-E values where the structure is observed in the in-situ data. Some of the MIPAS-E data points actually show values which are very similar to the low values observed between 20 and 25 km in the in-situ data. As this structure is caused by the presence of a filament of vortex air it is possible that this structure is not captured or not reproduced by the trajectory matching technique. While it is also possible that the vertical extend is partly dampened by the averaging kernels of MIPAS-E, the good agreement with some selected observations rather indicates that the discrepancy is caused by uncertainties in trajectory matching under such highly variable meteorological conditions.

AMTD
8, 7455–7489, 2015

Figure 2 shows the quantitative comparison for all cryosampler measurements available for this study: the mean differences (red lines in Fig. 2) and their scatter are compared with the mean error given from MIPAS-E database (blue line). Especially between 15 and 25 km the mixing ratio values of MIPAS-E are clearly overestimated. Above 25 km there is a good agreement according to the MIPAS-E error. In order to show the number of data which are available for the intercomparison the right hand side of the quantitative intercomparison plots show the number of data available per bin and the number of independent scans for which a sufficiently good match has been obtained.

As noted before the spectral resolution of MIPAS-E was degraded after January 2005. Therefore the absolute differences are compared for the period before and after January 2005 separately. Figure 3 displays the mean deviation between MIPAS-E-profiles and in-situ profiles for both time periods separately: the left panel presents the conclusions for earlier flights until 2003 (containing B39, B40 and B41) and the right panel for flights since 2005 (containing, B42, B43, B45 and B46). It is remarkable that the older flights obviously show significantly worse correlations than the younger ones, especially below ≈ 22 km with differences up to 400 ppb. The deviations in this part of the profile cannot be explained by the measurement accuracy of MIPAS-E. The validation based on the younger flights shows good to excellent correlations between MIPAS-E and balloon measurements. An exception is the altitude range of ≈ 21–25 km. This is mainly caused by the sharp structure observed during Flight B45 presented in Fig. 1. When disregarding the values between 20 and 25 km altitude from flight B45, the mean difference between MIPAS-E-profiles and the in-situ profiles becomes smoother (Fig. 4). In this case the deviation based on the CH_4-validation with the younger flights can be explained almost for the full profile range by the quoted uncertainty in the MIPAS-E retrieval (Fig. 4, right panel).

AMTD
8, 7455–7489, 2015

3.2 Validation of MIPAS-E-N_2O

The N_2O profile of flight B45 from the cryogenic whole air sampler is displayed in Fig. 5. It shows the same significant structure as observed for CH_4. This leads to N_2O mixing ratio values clearly overestimated by MIPAS-E in an altitude range between 20 and 25 km. Below 20 km the two N_2O-profiles fit together almost perfect. Above 25 km there is a tendency for MIPAS-E to underestimate the in-situ data. As in the case of CH_4 enhanced variability is observed in the matched MIPAS-E data. Again, as in the case of CH_4, the region with the strong vertical structure shows enhance variability in the MIPAS-E observations with some observations showing a similar structure as the in-situ data. The discrepancy is thus most probably not representative for MIPAS-E observations in this region. The quantitative N_2O validation based on all flights is displayed in Fig. 6. The most significant mean differences are located at an altitude of 20–25 km and are mainly caused by the sharp structure in the profile of B45. Above and below this altitude range the agreement is much better, so that differences between MIPAS-E- and in-situ observations can be explained by the stated uncertainty of the MIPAS-E values.

Figure 7 again distinguishes between high resolution (flights B39, B40 and B41) and low resolution measurements (flights B42, B43, B45 and B46) of MIPAS-E. For the validation based on the older (high resolution) flights between ≈ 13 and 21 km the deviations between N_2O mixing ratio values measured by satellite and balloon respectively are significantly higher than the stated MIPAS-E N_2O error, with MIPAS-E values consistently higher than the in-situ data. The younger low resolution data tend to overestimate the mixing ratios below 20 km. The overall reasonable agreement below 20 km is thus in case of N_2O in part due to an overestimation of N_2O mixing ratios in the high resolution and an underestimation in the low resolution data. In addition, MIPAS-E consistently underestimates the mixing ratio values at altitudes above ≈ 27 km for the older high resolution data set. In comparison the validation based on the younger flights with lower spectral resolution generally shows better agreement (especially above 25 km),

AMTD
8, 7455–7489, 2015

with the exception of the region between ≈ 21 and 25 km which is again explained by the special feature in the B45 data (Fig. 5). Figure 8 shows the differences for the entire data set and the low resolution data set when the region between 21 and 25 km from the flight B45 is eliminated from the data set. An overall display show the mean deviation is affected by the sharp structure.

3.3 Validation of MIPAS-E-CFC-12

The vertical structure of the CFC-12-profile for flight B45 (Fig. 9) looks similar to the profiles of CH_4- and N_2O which are displayed in Figs. 1 and 5 respectively. The altitude range including the dynamical feature shows large differences between the matched MIPAS-E data and the in-situ data. Again the variability in the matched MIPAS-E data is larger in the region of the dynamical feature indicating that the mismatch is most probably due to inaccuracies of the match technique applied here. In contrast to CH_4 and N_2O there is also a significant discrepancy below about 13 km, where the CFC-12 mixing ratios measured by MIPAS-E underestimate the in-situ data. Using all available flights the differences between MIPAS-E and in-situ data are mostly within the measuring error specified for MIPAS-E (Fig. 10). Especially above 25 km the agreement is excellent. Below ≈ 13 km the mixing ratio values are underestimated, most significantly in the lowest bin between 10 and 11 km. For the region below 20 km a very high variability is observed in the validation results as indicated by the large error bars which are substantially larger than the quoted uncertainty. As in the case of CH_4 and N_2O the combination of all data may not reveal all aspects of the validation. Figure 11 shows the difference between the validation based on the older (high resolution) flights and the younger (low resolution) ones respectively. For the validation based on the older flights (left panel) the mixing ratio values measured by MIPAS-E are overestimated below 20 km, whereas based on the younger flights (right panel) there is an underestimation. So for the combined validation displayed in Fig. 10 these two discrepancies nearly compensate each other. This is reflected in the large variability below 20 km shown in Fig. 10. Figure 11 (right panel) shows again a significant discrepancy in the 21–25 km

AMTD
8, 7455–7489, 2015

altitude region where the dynamical feature is observed in flight B45. Figure 12 again shows the result of eliminating this feature from the validation for the entire period (left panel) and the low resolution data after January 2005 (right panel). In both cases the results from the validation are very satisfactory above 20 km. Below 20 km the mean good agreement in the overall validation is again an effect of a cancellation of the overestimation for the early flights and the underestimation for the later flights.

3.4 Validation of MIPAS-E-CFC-11

CFC-11 is the shortest lived of all trace gases discussed here (SPARC, 2013). The vertical profile observed on 10 March 2009 (flight B45) is displayed in Fig. 13 in comparison to the matched satellite data. The strong dynamical feature observed in the profiles of N_2O, CH_4 and CFC-12 is much less obvious in the CFC-11 data of the cryogenic whole sampler. Upon close inspection higher mixing ratios of CFC-11 are indeed observed at 25 km (thus just above the dynamical feature) in comparison to the samples collected around 21 and 23 km altitude. The reason for this behaviour is that CFC-11 is nearly completely photolysed in this region of the stratosphere already, making it less sensitive to dynamical variability. The comparison in Fig. 13 does however reveal that the mixing ratios of CFC-11 are overestimated by the retrieval algorithm over the entire range of the profile. Even at altitudes where CFC-11 is no longer measured by the cryogenic whole sampler (i.e. the mixing ratio is below the detection limit of about 0.5 ppt), the retrieval yields several tens of ppt of CFC-11, which is clearly unrealistic. As can be seen in Fig. 14 the combined validation of CFC-11 shows the lowest quality in comparison to the validation of CH_4, N_2O and CFC-12. For the full altitude range the CFC-11 mixing ratio values are overestimated and not explainable with the uncertainty stated in the MIPAS-E data used here. The overestimation of the CFC-11 mixing ratios is obvious in both the older high resolution data and the younger low resolution data, although the difference are largest in the upper part of the profiles for the later data and in the lowest part of the earlier data. The differences between satellite and balloon mixing ratio cannot be explained with the measurement uncertainty.

AMTD
8, 7455–7489, 2015

4 Discussion and conclusion

The comparison of the results of in-situ measurements and satellite instruments is important in order to assess the quality of the satellite data. The data base available in this study for the validation of MIPAS-E operational retrievals (version 6.0) of CH_4, N_2O, CFC-12 and CFC-11 is rather small with only 7 flights, i.e. 7 vertical profiles from the in-situ observations. In addition the validation took place under different geophysical and meteorological conditions and the instrumental resolution of MIPAS-E was changed as of January 2005 due to technical problems, which requires additional attention as the spectral resolution will affect the retrieval results. The validation results are not always unambiguous, in particular significant differences are observed in the comparison with the high resolution and the low resolution data. Surprisingly the data after January 2005 (low resolution) seem to show a better agreement with the in-situ data. Above 20 km altitude there is a good agreement between both data sets within the errors given in the MIPAS-E retrieval for CH_4, N_2O and CFC-12. For the older high resolution data a significant underestimation of both CH_4 and N_2O in this retrieval version is observed above 25 km which can be on the order of 100 ppb of CH_4 and 30 ppb N_2O around 30 km altitude. An underestimation of the CFC-12 mixing ratios is also observed but this feature is closer to the uncertainty range given in the CFC-12 retrieval. In contrast to this we find a significant overestimation of mixing ratios of CH_4, N_2O and CFC-12 below 20 km, which may be as large as 300 ppb of CH_4, 40 ppb of N_2O and 50 ppt of CFC-12. In combination this should result in an overestimation of the vertical gradient of these three trace gases in the older high resolution data.

After elimination of a dynamical feature, which is probably not well caught in the trajectory matching, the younger low resolution data generally agree better with our in-situ data. Above 20 km there is generally a good agreement which is within the estimated uncertainty limits for CH_4, N_2O and CFC-12. For CH_4 a good agreement is also observed below 20 km, while there seems to be a tendency for an underestimation of the mixing ratios of N_2O (20 ppb at around 15 km) and also of CFC-12 (50 ppt at 10 km).

AMTD
8, 7455–7489, 2015

For CFC-11 the validation results show the clearest structure. The ESA version 6.0 retrieval of MIPAS-E clearly and significantly overestimates the CFC-11 mixing over the entire stratosphere both in the older high resolution and the younger low resolution data. This version of the CFC-11 retrieval cannot be recommended for scientific studies.

Acknowledgements. We would like to acknowledge Ingeborg Levin from University of Heidelberg for providing measurements of CH_4 and N_2O for the samples of the cryosampler. The validation flights were part of the Envisat validation programme and were funded through projects from ESA (ESRIN contract No. 20752/08/I-OL) and from the German research ministry (Grant No. 50EE0016 and 50EE0842). Operational Envisat data were provided by ESA.

References

Dlugokencky, E. J., Myers, R. C., Lang, P. M., Masarie, K. A., Crotwell, A. M., Thoning, K. W., Hall, B. D., Elkins, J. W., and Steele, L. P.: Conversion of NOAA atmospheric dry air CH_4 mole fractions to a gravimetrically prepared standard scale, J. Geophys. Res.-Atmos., 110, D18306, doi:10.1029/2005JD006035, 2005.

Engel, A., Schmidt, U., and Stachnik, R. A.: Partitioning between chlorine reservoir species deduced from observations in the arctic winter stratosphere, J. Atmos. Chem., 27, 107–126, 1997.

Engel, A., Möbius, T., Haase, H.-P., Bönisch, H., Wetter, T., Schmidt, U., Levin, I., Reddmann, T., Oelhaf, H., Wetzel, G., Grunow, K., Huret, N., and Pirre, M.: Observation of mesospheric air inside the arctic stratospheric polar vortex in early 2003, Atmos. Chem. Phys., 6, 267–282, doi:10.5194/acp-6-267-2006, 2006.

Engel, A., Atlas, E. L., Bernath, P. F., Bönisch, H., Brown, A., Laube, J. C., Minschwaner, K., Montzka, S. A., O'Doherty, S., Prinn, R. G., Rigby, M., Schauffler, S., Volk, C. M., and Yvon-Lewis, S. A.: Inferred Lifetimes from Observed Trace-Gas Distributions, in: SPARC Report N° 6 (2013) Lifetimes of Stratospheric Ozone-Depleting Substances, Their Replacements, and Related Species, edited by: Ko, M. K. W., Newman, P. A., Reimann, S., and Strahan, S. E., 2013.

AMTD
8, 7455–7489, 2015

Fischer, H., Birk, M., Blom, C., Carli, B., Carlotti, M., von Clarmann, T., Delbouille, L., Dudhia, A., Ehhalt, D., Endemann, M., Flaud, J. M., Gessner, R., Kleinert, A., Koopman, R., Langen, J., López-Puertas, M., Mosner, P., Nett, H., Oelhaf, H., Perron, G., Remedios, J., Ridolfi, M., Stiller, G., and Zander, R.: MIPAS: an instrument for atmospheric and climate research, Atmos. Chem. Phys., 8, 2151–2188, doi:10.5194/acp-8-2151-2008, 2008.

Grunow, K.: Anwendung von Trajektorien zur Envisat-Validierung und zur Untersuchung der Luftmassenherkunft in der Stratosphäre, PhD thesis, Free University Berlin, Berlin, 2009.

Hall, B. D., Dutton, G. S., and Elkins, J. W.: The NOAA nitrous oxide standard scale for atmospheric observations, J. Geophys. Res.-Atmos., 112, D09305, doi:10.1029/2006JD007954, 2007.

Hoffmann, L., Kaufmann, M., Spang, R., Müller, R., Remedios, J. J., Moore, D. P., Volk, C. M., von Clarmann, T., and Riese, M.: Envisat MIPAS measurements of CFC-11: retrieval, validation, and climatology, Atmos. Chem. Phys., 8, 3671–3688, doi:10.5194/acp-8-3671-2008, 2008.

Hoker, J., Obersteiner, F., Bönisch, H., and Engel, A.: Comparison of GC/time-of-flight MS with GC/quadrupole MS for halocarbon trace gas analysis, Atmos. Meas. Tech., 8, 2195–2206, doi:10.5194/amt-8-2195-2015, 2015.

Kellmann, S., von Clarmann, T., Stiller, G. P., Eckert, E., Glatthor, N., Höpfner, M., Kiefer, M., Orphal, J., Funke, B., Grabowski, U., Linden, A., Dutton, G. S., and Elkins, J. W.: Global CFC-11 (CCl_3F) and CFC-12 (CCl_2F_2) measurements with the Michelson Interferometer for Passive Atmospheric Sounding (MIPAS): retrieval, climatologies and trends, Atmos. Chem. Phys., 12, 11857–11875, doi:10.5194/acp-12-11857-2012, 2012.

Laube, J. C., Engel, A., Bönisch, H., Möbius, T., Worton, D. R., Sturges, W. T., Grunow, K., and Schmidt, U.: Contribution of very short-lived organic substances to stratospheric chlorine and bromine in the tropics – a case study, Atmos. Chem. Phys., 8, 7325–7334, doi:10.5194/acp-8-7325-2008, 2008.

Levin, I., Glatzel-Mattheier, H., Marik, T., Cuntz, M., Schmidt, M., and Worthy, D. E.: Verification of German methane emission inventories and their recent changes based on atmospheric observations, J. Geophys. Res.-Atmos., 104, 3447–3456, 1999.

Lueb, R. A., Ehhalt, D. H., and Heidt, L. E.: Balloon-borne low-temperature air sampler, Rev. Sci. Instrum., 46, 702–705, 1975.

Manney, G. L., Santee, M. L., Rex, M., Livesey, N. J., Pitts, M. C., Veefkind, P., Nash, E. R., Wohltmann, I., Lehmann, R., Froidevaux, L., Poole, L. R., Schoeberl, M. R., Haffner, D. P.,

AMTD
8, 7455–7489, 2015

Davies, J., Dorokhov, V., Gernandt, H., Johnson, B., Kivi, R., Kyro, E., Larsen, N., Levelt, P. F., Makshtas, A., McElroy, C. T., Nakajima, H., Parrondo, M. C., Tarasick, D. W., von der Gathen, P., Walker, K. A., and Zinoviev, N. S.: Unprecedented Arctic ozone loss in 2011, Nature, 478, 469–475, 2011.

Minschwaner, K., Hoffmann, L., Brown, A., Riese, M., Müller, R., and Bernath, P. F.: Stratospheric loss and atmospheric lifetimes of CFC-11 and CFC-12 derived from satellite observations, Atmos. Chem. Phys., 13, 4253–4263, doi:10.5194/acp-13-4253-2013, 2013.

Montzka, S. A., Butler, J. H., Hall, B. D., Mondeel, D. J., and Elkins, J. W.: A decline in tropospheric organic bromine, Geophys. Res. Lett., 30, 1826, doi:10.1029/2003GL017745, 2003.

Naujokat, B. and Grunow, K.: The stratospheric arctic winter 2002/03: balloon flight planning by trajectory calculations, in: 16th Esa Symposium on European Rocket and Balloon Programmes and Related Research, Proceedings, 530, 421–425, 2003.

Payan, S., Camy-Peyret, C., Oelhaf, H., Wetzel, G., Maucher, G., Keim, C., Pirre, M., Huret, N., Engel, A., Volk, M. C., Kuellmann, H., Kuttippurath, J., Cortesi, U., Bianchini, G., Mencaraglia, F., Raspollini, P., Redaelli, G., Vigouroux, C., De Mazière, M., Mikuteit, S., Blumenstock, T., Velazco, V., Notholt, J., Mahieu, E., Duchatelet, P., Smale, D., Wood, S., Jones, N., Piccolo, C., Payne, V., Bracher, A., Glatthor, N., Stiller, G., Grunow, K., Jeseck, P., Te, Y., and Butz, A.: Validation of version-4.61 methane and nitrous oxide observed by MIPAS, Atmos. Chem. Phys., 9, 413–442, doi:10.5194/acp-9-413-2009, 2009.

Plumb, R. A. and Ko, M. K. W.: Interrelationships between mixing ratios of long lived stratospheric constituents, J. Geophys. Res.-Atmos., 97, 10145–10156, 1992.

Schmidt, M., Glatzel-Mattheier, H., Sartorius, H., Worthy, D. E., and Levin, I.: Western European N_2O emissions: a top-down approach based on atmospheric observations, J. Geophys. Res.-Atmos., 106, 5507–5516, 2001.

Schwarzenberger, T.: Validierung von MIPAS-Envisat-Messungen mithilfe von in-situ Ballonmessungen, Master thesis, Goethe University Frankfurt, Frankfurt am Main, Germany, 2014.

SPARC: SPARC Report on the Lifetimes of Stratospheric Ozone-Depleting Substances, Their Replacements, and Related Species Rep., SPARC Report No. 6, WCRP-15/2013, SPARC, 2013.

Stiller, G. P., von Clarmann, T., Höpfner, M., Glatthor, N., Grabowski, U., Kellmann, S., Kleinert, A., Linden, A., Milz, M., Reddmann, T., Steck, T., Fischer, H., Funke, B., López-Puertas, M., and Engel, A.: Global distribution of mean age of stratospheric air from MIPAS SF_6 measurements, Atmos. Chem. Phys., 8, 677–695, doi:10.5194/acp-8-677-2008, 2008.

AMTD
8, 7455–7489, 2015

Vigouroux, C., De Mazière, M., Errera, Q., Chabrillat, S., Mahieu, E., Duchatelet, P., Wood, S., Smale, D., Mikuteit, S., Blumenstock, T., Hase, F., and Jones, N.: Comparisons between ground-based FTIR and MIPAS N_2O and HNO_3 profiles before and after assimilation in BASCOE, Atmos. Chem. Phys., 7, 377–396, doi:10.5194/acp-7-377-2007, 2007.

AMTD
8, 7455–7489, 2015

Table 1. Acronym, number of airsamples, altitude range, location and flight date of the cryosampler-flights considered for the validation. The acronym BXX refers to flight nr. XX of the balloon borne whole air samplers. University Frankfurt operates two nearly identical cryogenic whole air samplers allowing to perform two flights during a campaign.

Acronym	Number of airsamples	Altitude range	Location	Flight date
B39	14	12.2–32.4 km	44° N, Aire sur l'Adour, France	24 Sep 2002
B40	13	11.2–30.4 km	68° N, Kiruna, Sweden	6 Mar 2003
B41	10	13.3–28.9 km	68° N, Kiruna, Sweden	9 Jun 2003
B42	11	15.2–34.0 km	5° S, Teresina, Brazil	8 Jun 2005
B43	14	15.2–33.6 km	5° S, Teresina, Brazil	25 Jun 2005
B45	11	10.3–31.8 km	68° N, Kiruna, Sweden	10 Mar 2009
B46	8	12.5–23.3 km	68° N, Kiruna, Sweden	1 Apr 2011

AMTD
8, 7455–7489, 2015

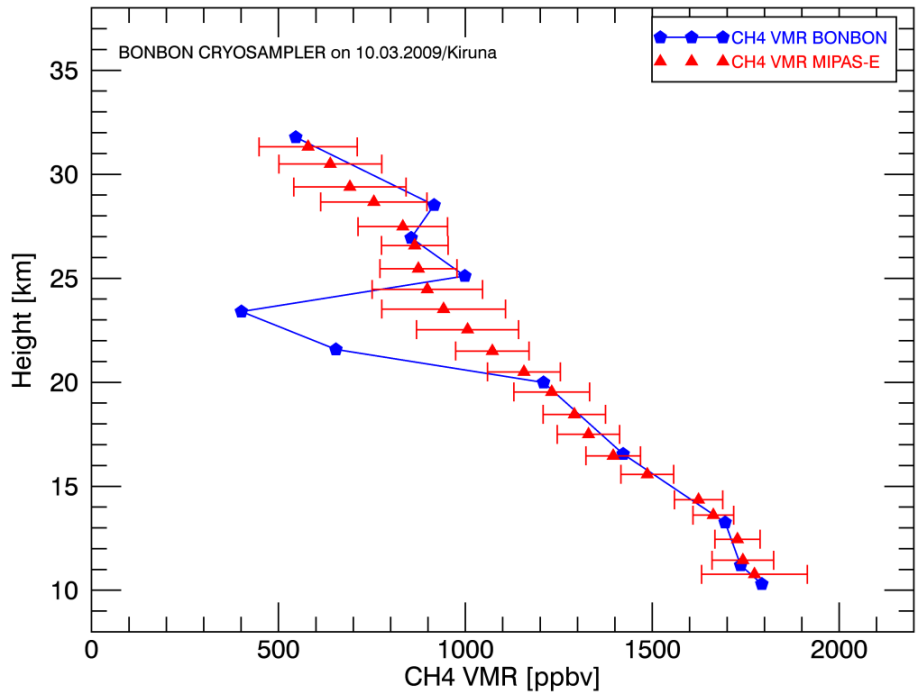

Figure 1. Comparison of CH_4-profile retrieved from B45 (1 April 2011, from Kiruna Sweden, 68° N) and the related mean MIPAS-E-profile based on the trajectory matching results. Blue dots: cryosampler measurements. Blue line: interpolated CH_4-profile from cryosampler (BONBON). Red triangle: mean CH_4 mixing ratio values of MIPAS-E. Red error bars: standard deviation of matched Envisat data.

AMTD
8, 7455–7489, 2015

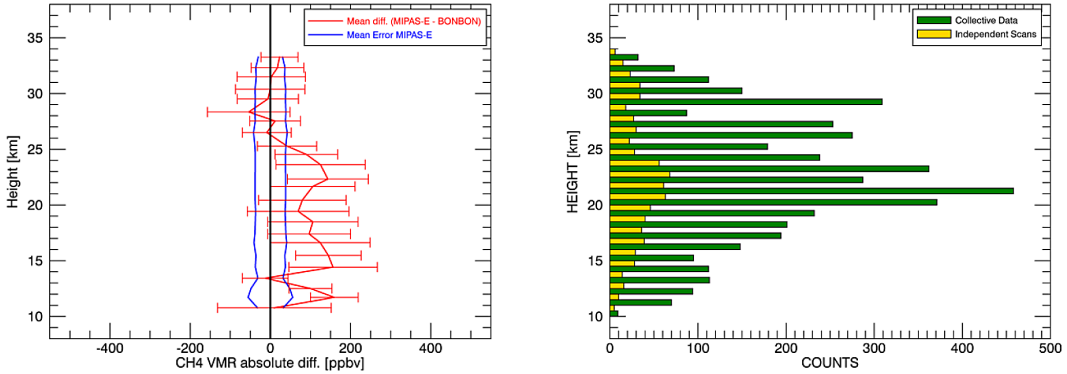

Figure 2. Left panel: CH_4-Validation based on all cryosampler (BONBON)-flights considered in this study. Red line: interpolated mean difference between MIPAS-E- and cryosampler-mixing ratio values. Red error bars: mean standard deviation of the difference between MIPAS-E- and cryosampler-mixing ratio value interpolated to the respective altitude. Blue line: interpolated mean error for CH_4 mixing ratio values from MIPAS-E. Right panel: corresponding database of MIPAS-E. Green bars: total nr. of matches. Yellow bars: nr. of independent scans which are matched.

AMTD
8, 7455–7489, 2015

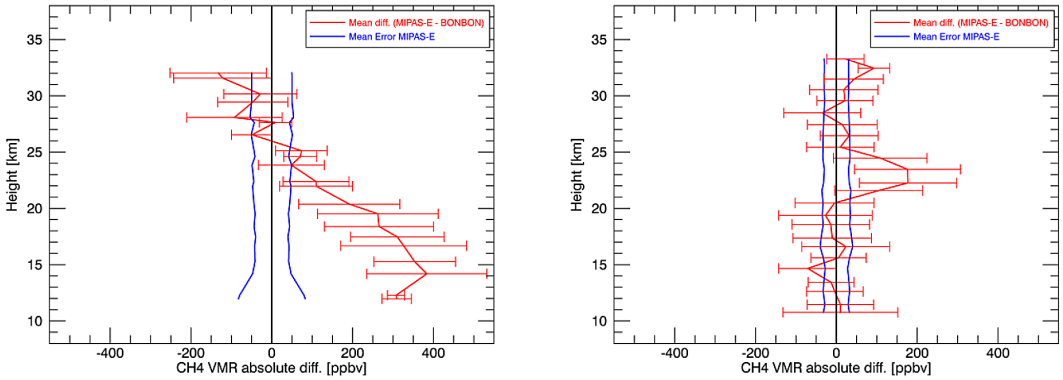

Figure 3. Left panel: CH_4-Validation based on cryosampler (BONBON)-flights B39, B40 and B41. Red line: interpolated Mean difference between MIPAS-E- and croysampler-mixing ratios. Red error bars: mean standard deviation of the difference between MIPAS-E- and cryosampler-mixing ratios for the respective altitude range. Blue line: interpolated mean error for CH_4 mixing ratio values from MIPAS-E database. Right panel: CH_4-validation based on cryosampler-flights B42, B43, B45 and B46. Red line: interpolated mean difference between MIPAS-E- and cryosampler-mixing ratios. Red error bars: mean standard deviation of the difference between MIPAS-E- and cryosampler-mixing ratios for the respective altitude range. Blue line: interpolated Mean error for CH_4 mixing ratios from MIPAS-E database.

AMTD
8, 7455–7489, 2015

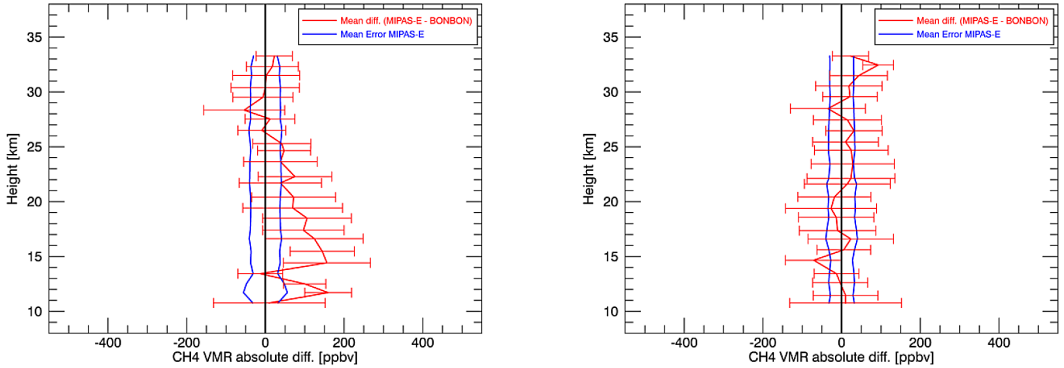

Figure 4. Without data range containing the meteorological feature in profile B45. Left panel: CH_4-Validation based on all cryosampler (BONBON)-flights considered in this study. Red line: interpolated mean difference between MIPAS-E- and cryosampler-mixing ratio values. Red error bars: mean standard deviation of the difference between MIPAS-E- and cryosampler-mixing ratio value for the respective altitude range. Blue line: interpolated mean error for CH_4 mixing ratio values from MIPAS-E database. Right panel: CH_4-validation based on cryosampler-flights B42, B43, B45 and B46. Red line: interpolated mean difference between MIPAS-E- and cryosampler-mixing ratio values. Red error bars: mean standard deviation of the difference between MIPAS-E- and cryosampler-mixing ratio value for the respective altitude range. Blue line: interpolated mean error for CH_4 mixing ratio values from MIPAS-E database.

AMTD
8, 7455–7489, 2015

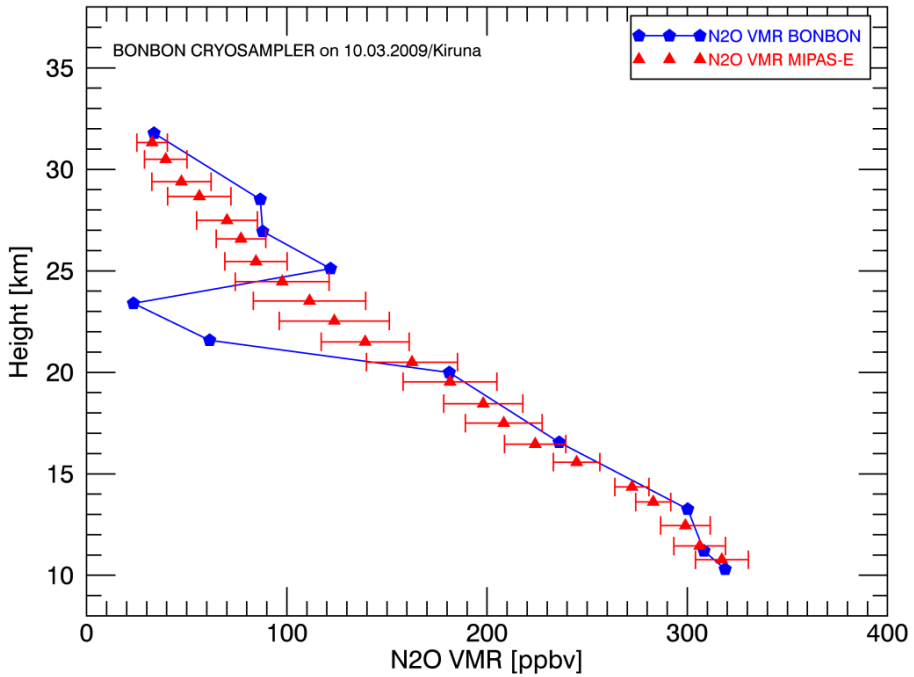

Figure 5. As Fig. 1, but instead of CH_4 now N_2O.

AMTD
8, 7455–7489, 2015

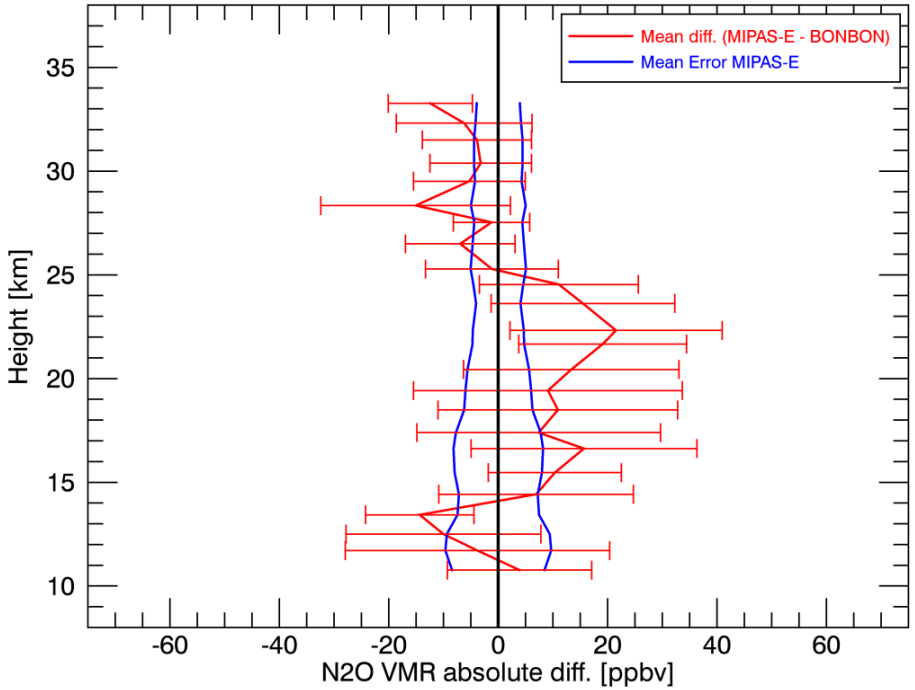

Figure 6. As Fig. 2, but instead of CH_4 now N_2O.

AMTD
8, 7455–7489, 2015

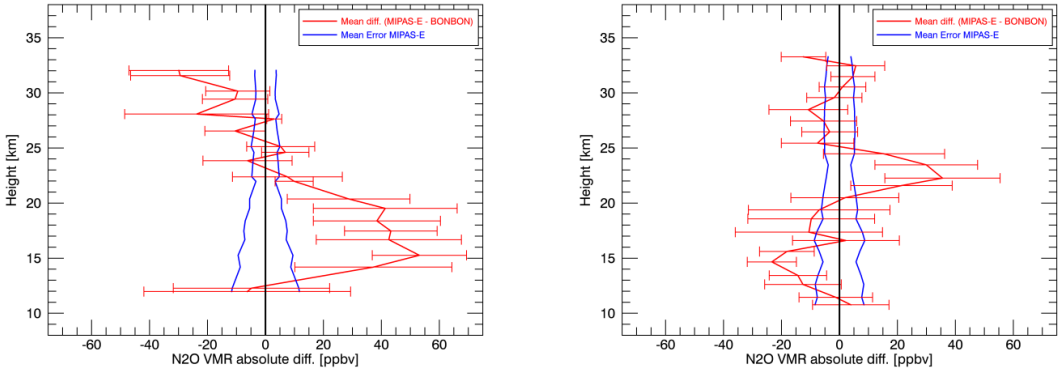

Figure 7. As Fig. 3, but instead of CH_4 now N_2O.

AMTD
8, 7455–7489, 2015

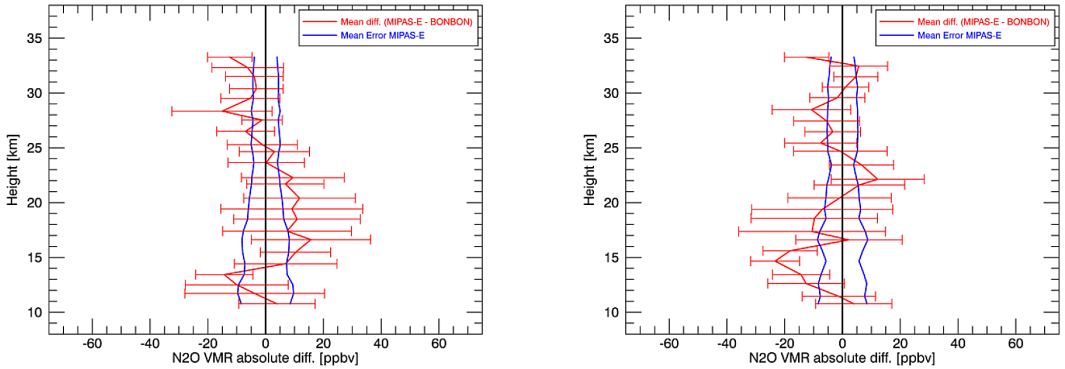

Figure 8. As Fig. 4, but instead of CH_4 now N_2O.

AMTD
8, 7455–7489, 2015

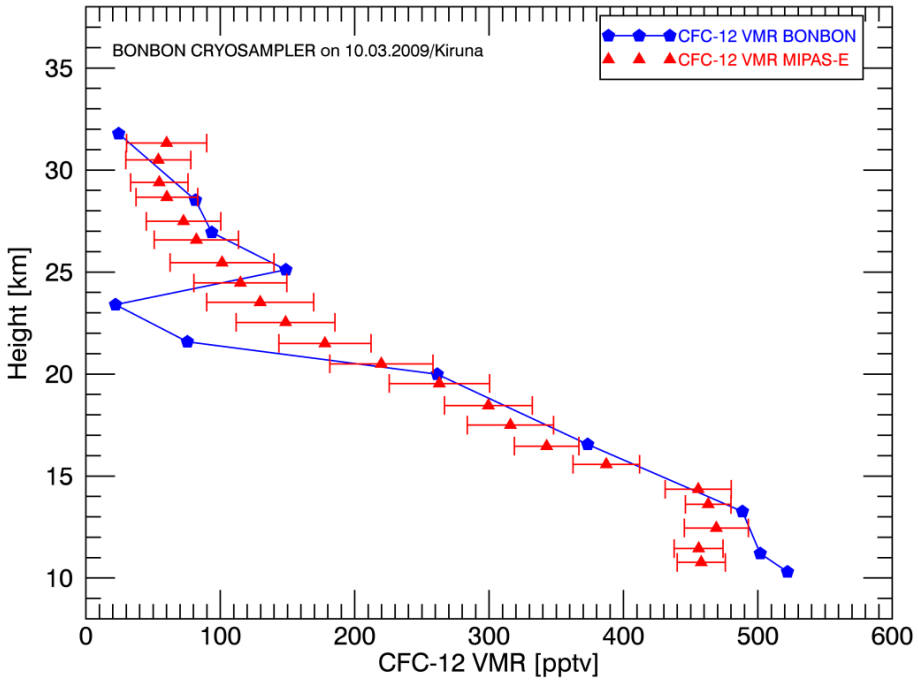

Figure 9. As Fig. 1, but instead of CH_4 now CFC-12.

AMTD
8, 7455–7489, 2015

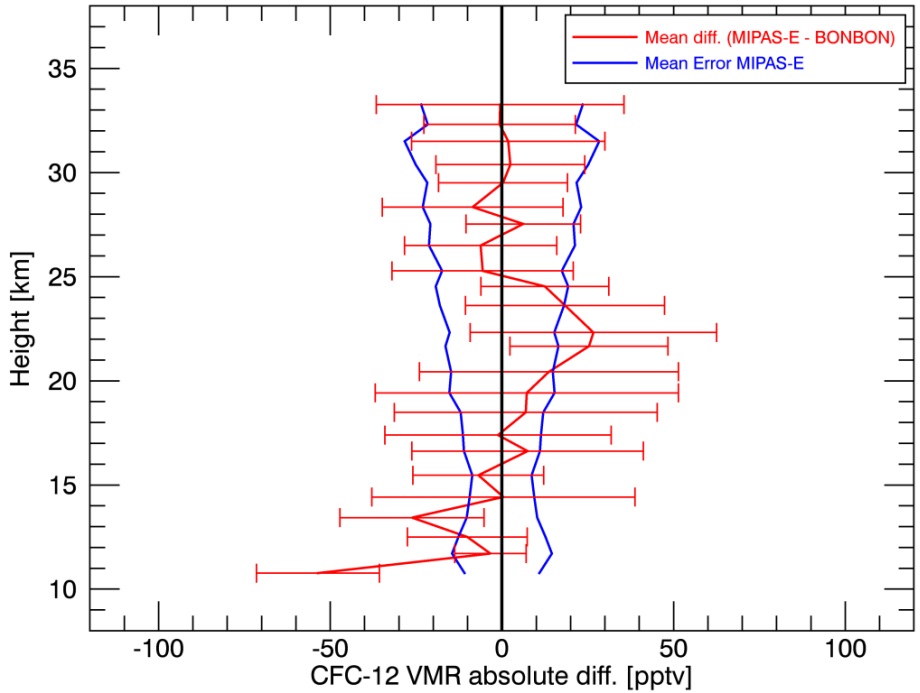

Figure 10. As Fig. 2 but instead of CH_4 now CFC-12.

AMTD
8, 7455–7489, 2015

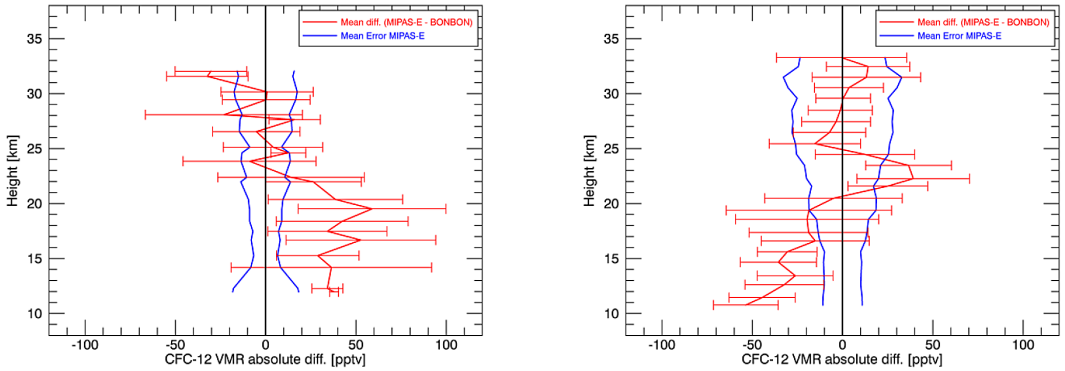

Figure 11. As Fig. 3, but instead of CH_4 now CFC-12.

AMTD
8, 7455–7489, 2015

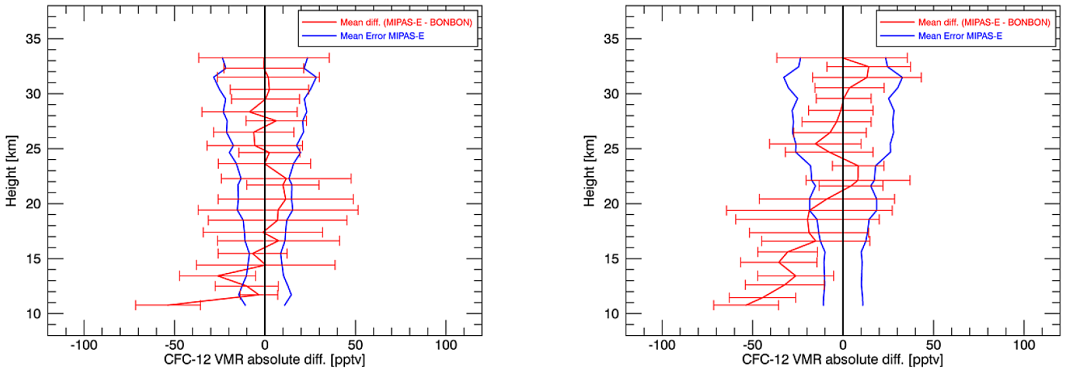

Figure 12. As Fig. 4, but instead of CH_4 now CFC-12.

AMTD
8, 7455–7489, 2015

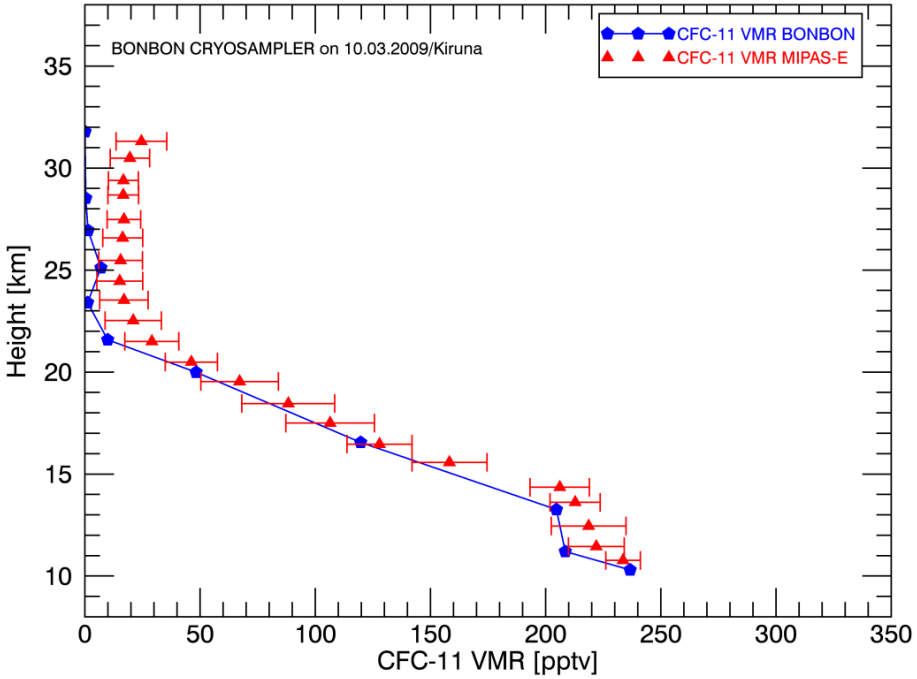

Figure 13. As Fig. 1, but instead of CH_4 now CFC-11.

AMTD
8, 7455–7489, 2015

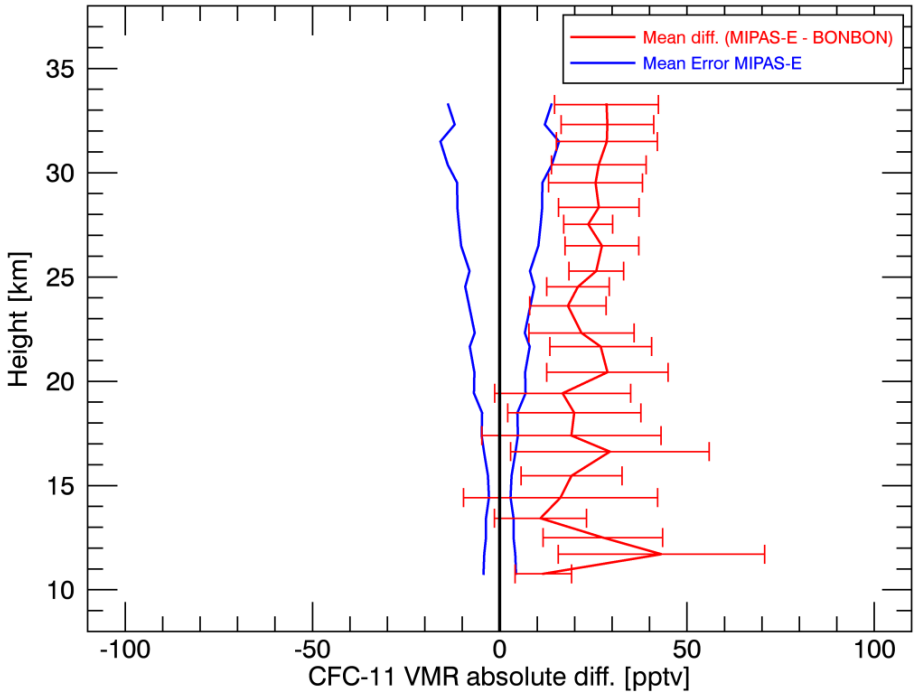

Figure 14. As Fig. 2, but instead of CH_4 now CFC-11.

AMTD
8, 7455–7489, 2015

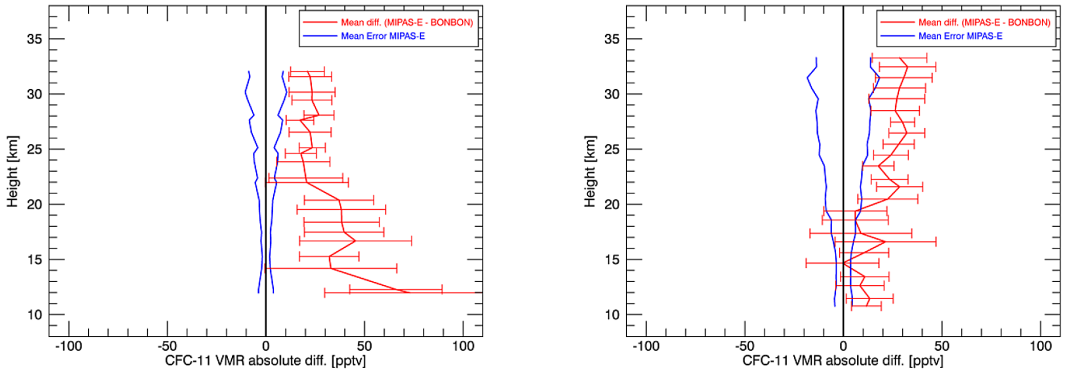

Figure 15. As Fig. 3, but instead of CH_4 now CFC-11.

AMTD
8, 7455–7489, 2015